Hindawi
Advances in Materials Science and Engineering
Volume 2017, Article ID 3849648, 10 pages
https://doi.org/10.1155/2017/3849648

Research Article

Time-Dependent Variations in Structure of Sheep Wool Irradiated by Electron Beam

Zuzana Hanzlíková,[1] Michael Kenneth Lawson,[1] Peter Hybler,[2] Marko Fülöp,[2] and Mária Porubská[1]

[1]*Department of Chemistry, Faculty of Natural Sciences, Constantine the Philosopher University in Nitra, Tr. A. Hlinku 1, 94974 Nitra, Slovakia*
[2]*University Centre of Electron Accelerators in Trenčín, Slovak Medical University, Limbová 12, 83303 Bratislava, Slovakia*

Correspondence should be addressed to Mária Porubská; mporubska@ukf.sk

Received 8 November 2016; Revised 18 January 2017; Accepted 16 February 2017; Published 16 March 2017

Academic Editor: Carlo Santulli

Wool scoured in tap water with no special degreasing and containing a balanced humidity responding to usual laboratory conditions was irradiated by accelerated electron beam in the range of 0–350 kGy dose. Time variations of the wool structure were measured using FTIR, Raman, and EPR spectroscopy. The aim was to determine whether preexposure treatment of the wool, as well as postexposure time, affects the properties of the irradiated wool. Reactive products such as S-sulfonate, cystine monoxide, cystine dioxide, cysteic acid, disulphides, and carboxylates displayed a considerable fluctuation in quantity depending on both the absorbed dose and time. Mutual transformations of S-oxidized products into cysteic acid appeared to be faster than those in dry and degreased wool assuming that the present humidity inside the fibres is decisive as an oxygen source. EPR results indicated a longer lifetime for free radicals induced by lower doses compared with the radicals generated by higher ones. The pattern of the conformational composition of the secondary structure (α-helix, β-sheet, random, and residual conformations) also showed a large variability depending on absorbed dose as well as postexposure time. The most stable secondary structure was observed in nonirradiated wool but even this showed a small but observable change after a longer time, too.

1. Introduction

Sheep wool is a valuable material with unique properties used traditionally and especially in the garment industry. Since only wool of high quality is utilized in the textile industry, unprocessed wool often regrettably becomes waste at loading depots. Thermal insulation of buildings using sheep wool is not too widespread due to the serious competitors in this field, that is, expanded polystyrene and mineral wool.

Sheep wool is based on keratin containing more than 170 different proteins and polypeptides composed of different α-amino acids structured in α-helical form, mostly cysteine (7–20%) [1–4] along with a small quantity of lipids (0.1%) and mineral salts (0.5%) [5, 6]. Keratin fibres are chemically inhomogeneous and the mixture of different polypeptides is complex [7]. So-called hard keratin inherent in wool, hair, feathers, nails, and horns contains more than 3% of sulphur in mass [8]. The α-keratin dimer is stabilized by hydrogen bonds as well as inter- and intramolecular disulphide bonds which are responsible for a compact three-dimensional stable structure [9, 10]. Keratin is reactive, biocompatible, and biodegradable [11].

Efforts to modify wool in order to improve textile properties have involved, besides chemical methods, procedures such as plasma treatment [12–16], corona discharge [17], microwave irradiation [18], or UV radiation [19]. Plasmatic treatment of the wool surface is the most documented among the mentioned modifications. This process can change the surface properties of wool without major modification of the properties inside the fibre [20] and chemical composition of plasma treated surface is dependent on the character of the surrounding gaseous atmosphere [21, 22]. If plasma atmosphere involves combination of several gases (nitrogen, air, and water vapour), an attentive control of reproducible

composition of the used atmosphere can be problematic. Some difficulties can be expectable when such process should be continual and efficient. Microwave treatment showed only a little improvement in fibre dyeability due to generation mild wrinkles on the fibre surface without chemical change. Application of UV radiation, as is well known, generates toxic ozone as by-product when irradiation is carried out on air. In general, there is a lack of information on industrial applications of the above-mentioned processes utilizable in the textile industry.

Within last decades, radiation technics including electron irradiation have been used to generate free radicals in synthetic polymers. Recently, as the first we published a study on effect of accelerated electron beam on sheep wool [23]. The irradiation being "dry" and nonwaste technology is of great merit, since accelerated electron beam penetrates whole fibre volume modifying it. This is a considerable advantage in comparison with the above-mentioned technics. By contrast, continual irradiation in electron accelerator is feasible very well and it has been applied in industry (cross-linking plastics, sterilization of medical items, etc.). Although the modification of sheep wool by electron beam is in phase of beginning research only, the actual results have indicated possible use of such wool for specific nontextile purposes due to enhanced sorption properties [24]. However, volume of necessary knowledge is still scarce. That is why continuation in the research is expected.

In the first study [23], the examined wool was degreased and kept dry in a desiccator before electron irradiation. Related changes in primary and secondary structure were analysed after a 9-day time lapse after irradiation showing considerable variations in the monitored parameters. Depending on the absorbed dose, the following indicators were subjected to monitoring: functional groups involving sulphur, hydrocarbons, portions of α-helical, β-sheet, and random conformations in the secondary structure, and thermal and mechanical properties. In this work, we focused on wool scoured in water with no special degreasing and drying out before being exposed in order to enhance our knowledge about processes occurring due to electron beam irradiation. Such wool contained balanced humidity responding to usual laboratory conditions without targeted air-conditioning. Time variations of the wool structure were measured using FTIR, Raman, and EPR spectroscopy with the aim of finding out whether preexposure treatment of the wool as well as postexposure time affects properties of the irradiated wool.

2. Materials and Methods

2.1. Sample Preparation. The sheep wool was taken directly from sheep-shearing of a Tsigai-Suffolk crossbreed bred in Middle Slovakia. The fleece was not selected regarding the site taken from the part of the sheep's body and the fibre thickness was in the range of 27–33 μm. Crude impurities including excremental scraps were removed from the wool manually. Then the wool was severalfold scoured in warmish tap water until the rinse water was clean. Such precleaned material of a mass of about 12 g was put into a netted pouch and washed in tap water tempered to 40°C using an ultrasonic bath of 5 litres in volume during 2 × 10 min cycles and the water was exchanged in each washing cycle. Afterwards, the pouch was removed and hung on a laboratory stand to drain the trapped water thoroughly. Finally, the sample was dried in a laboratory oven at 40°C for 24 h and then put into an unsealed polyethylene bag and kept under usual laboratory conditions.

2.2. Sample Irradiation. The irradiation of the samples was carried out as described in a previous paper [23]. The doses applied were 0-16-25-40-63-117-170-250-350 kGy repeating 100 kGy cycles plus needed supplementing dose, if necessary. Between individual irradiation cycles, the samples were allowed to cool down for 30 minutes to maintain a temperature below 50°C. The absorbed doses were checked dosimetrically by radiochromic foils B3 using spectrometer GENESYS 20.

The irradiated samples were kept in unsealed polyethylene bags put in carton boxes under usual laboratory conditions.

The first spectral measurement was carried out 4 days after the irradiation and the next ones were within selected time intervals.

2.3. Spectral Measurement. For FTIR spectra measurement, the samples were deposited on a steel support and spread to form a thin layer. FTIR spectrometer Nicolet 6700 with a Continuum microscope was employed to take the spectra. FTIR spectra were collected over a 650–4000 cm^{-1} range, with a spectral resolution of 8 cm^{-1} and with 128 scans on average. Since infrared signals of S-compounds are rather weak, the collected FTIR spectra were converted to second-order derivative spectra; the related signals were read and divided by the signal for reference ethyl group at wavenumber of 2849 cm^{-1} (CH_2 symmetric vibrations). Comparison of those ratios with corresponding ratios of nonirradiated wool provided data on the relative content of the analysed components.

The Raman spectra were measured using FT-Raman spectrometer Nicolet NXR 9650 with a MicroStage adapter containing an integrated CCD camera to measure microsamples with measuring trace of 50 μm and enabling area survey with exciting wavelength of 1064 nm. To prevent catching fire during measurement, the wool was moulded into a compact structure applying a force of 70–80 kN by a hydraulic press equipped with membrane vacuum pump. The source of exciting radiation was Nd:YAG laser (532 nm) with optimized power to attain a quality spectrum and avoid the risk of the sample catching fire. The spectra were taken in the range of 400–4000 cm^{-1} and for qualitative analysis. Amide I band (1653 cm^{-1}, valence vibration) was used as reference band. No second-order derivation was used for Raman spectra processing.

Spectra corresponding to each absorbed dose were taken from three independent fibre samples and the corresponding relative deviations for measured absorbance data did not exceed 5% in average.

Table 1: Characteristic wavenumbers of functional groups for native wool used in FTIR and Raman spectroscopy [25, 26].

Characteristic group	Structure	$\tilde{\nu}$ (cm^{-1})
FTIR spectrometry		
S-sulfonate (Bunte salt)	-S-SO_3^--	1022
Cysteic acid	-SO_3^--	1044
Cystine monoxide	-SO-S-	1075
Cystine dioxide	-SO_2-S-	1128
Carboxylate	-COO^-	1389
Ethyl group, internal reference band	-CH_2-	2849
Raman spectrometry		
Disulfide bond	-S-S-	500–550
Amide I, internal reference band	-N-H	1653

Table 2: Wavenumbers for estimation of secondary structure conformation [27].

Amide II band, -CONH- group (1500–1600) cm^{-1}	Conformation
1545	α-Helix
1540	Random
1530	β-Sheet

Both FTIR and Raman spectra were processed using the OMNIC software, version 7.3. Vibration bands are listed in Tables 1 and 2.

EPR spectra were taken using Bruker EMX plus spectrometer operating at X band (9,4 GHz) at room temperature with 100 kHz field modulation. The g-factors were quoted with an uncertainty of 0.0001 using an internal reference standard marker containing 1,1-diphenyl-2-picrylhydrazyl built into the EPR spectrometer. Special thin cylindrical quartz tubes were used for the measurements. At each experiment, the sample mass was constant and that was reproducibly inserted into the tube. The EPR signal-to-noise ratio was improved using multiple scans. The spectra were processed with the commercially available software SimFonia (Bruker).

3. Results and Discussion

3.1. FTIR and Raman Spectral Measurements. Changes in the chemical structure observed through FTIR and Raman spectroscopy were monitored within 4 months after 4, 88, and 123 days after irradiation (Figures 1–6). As is evident in Figure 1, each dose gave a different pattern of composition regarding the functional groups.

In comparison with the other wool (industrially scoured with fibre thickness of 22–27 μm) which was prior to the irradiation degreased by Soxhlet dichloromethane extraction, dried and kept in desiccator until irradiation in the same accelerator [23], it is evident that development of analogous parameters is considerably different. The differences between them are observable despite comparable times of the first spectral measurements from the irradiation (9 days for the degreased dry wool and 4 days for the water scoured, resp.). While the development and fluctuating S-sulfonate

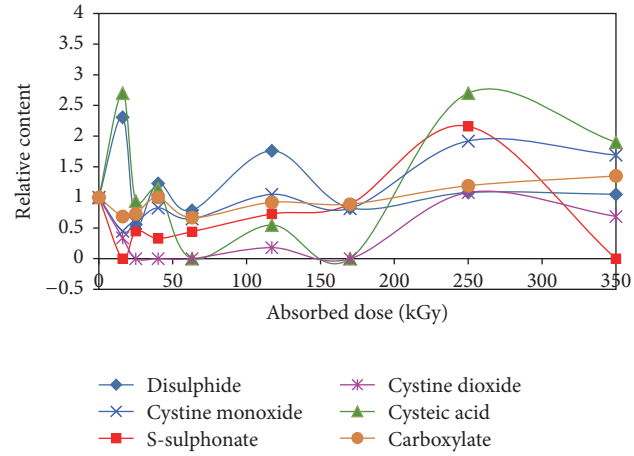

Figure 1: Variation of relative content in disulphides, S-sulfonate, cysteic acid, cystine monoxide, cystine dioxide, and carboxylates in the wool with absorbed dose 4 days after electron beam irradiation.

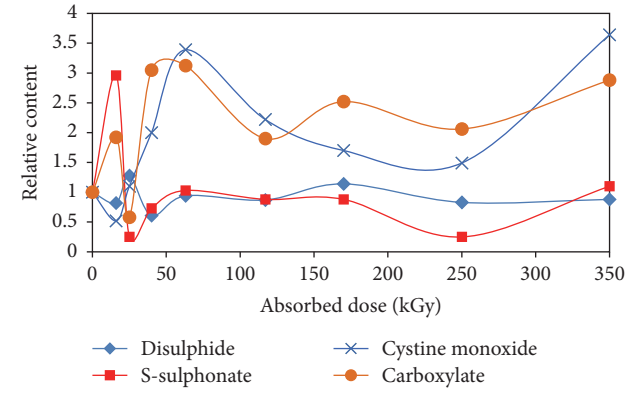

Figure 2: Development of relative content of disulphides, S-sulfonate, cystine monoxide, and carboxylates 88 days after electron beam irradiation.

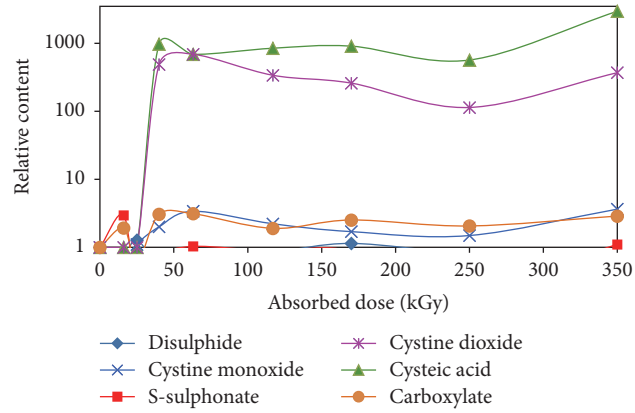

Figure 3: Development of relative content of cystine dioxide and cysteic acid along other species in the wool with absorbed dose 88 days after electron beam irradiation.

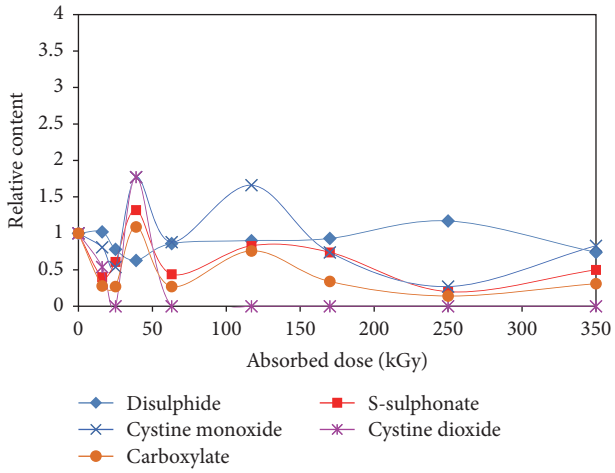

FIGURE 4: Development of relative content of disulphides, S-sulfonate, cysteine monoxide, cysteine dioxide, and carboxylates in the wool with absorbed dose 123 days after electron beam irradiation.

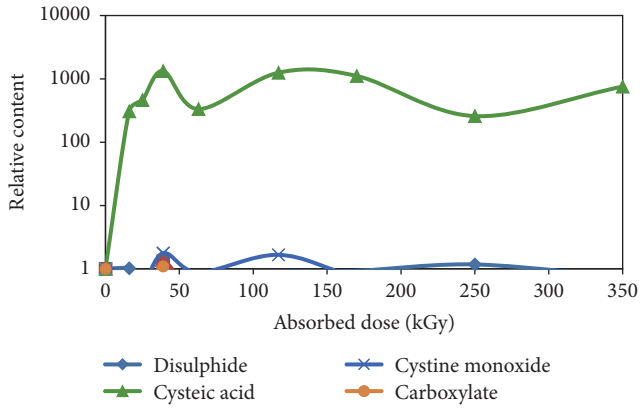

FIGURE 5: Development of relative content of cysteic acid in the wool with absorbed dose 123 days after electron beam irradiation.

was dominant almost to 200 kGy, it was then transformed into other S-oxidized species (namely, into cystine dioxide and cysteic acid) in the dry degreased wool; the wool scoured by water shows that relative content increased over an initial value only for cysteic acid and disulphides within the same range of doses. Doses above 200 kGy in the dry degreased wool generated only cysteic acid and cystine dioxide and any S-sulfonate or cysteine monoxide was no longer found [23], while in the water scoured wool cysteic acid, cystine dioxide, and S-sulfonate were detected. However, the last was no longer found at the highest dose of 350 kGy.

A common feature for both degreased and water scoured wools is a considerable fluctuation of the analysed components with absorbed dose. Being the generated species of polar character, the correspondent surface energy of the fibres should grow. This parameter was really determined in the degreased and water scoured wool samples [28]. It was found that the surface energy increased immediately already after the lowest dose and became stable from 100 kGy despite the fact that the content of polar groups continued to increase

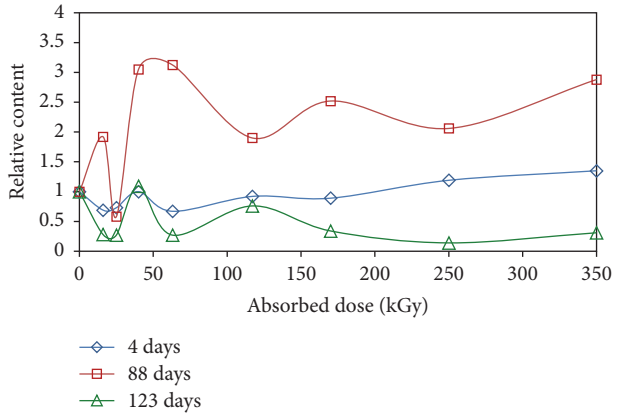

FIGURE 6: Variation of relative carboxylate content in the wool with absorbed dose; time data mean lapse from the irradiation.

in the bulk. It indicates the ultimate presence of whatever polar groups coming from already oxidized and transformed species situated at the available surface area regardless of the next doses' effect. The measured surface energy as complex indicator reflects conditions only at the fibre surface and, in addition, could not specify structural composition of the surface polar groups. Therefore, in the presented study, such measuring was omitted as not much informative factor.

We assume that the main reason of the differences in individual structural changes for both wools is not their different origin but the different humidity value as an oxygen source inside wool. It can be said that higher humidity content in irradiated wool suggests earlier cysteic acid generation compared with the dry and degreased one. Our expectation of decreasing disulphide groups already at starting doses based on low -S-S- binding energy (214 kJ/mol) [29] was not met (Figure 1). On the contrary, the -S-S- content increased variably and became stabilized around the initial level just beyond 170 kGy. The course of the dependence indicates that this growth for 117 kGy dose has occurred at the expense of decreasing representation of the other S-oxidized species. This means that during the absorption of the dose some reduction processes had to occur, which is rather surprising and unclear so far. The disulphide content was measured using a method (Raman) independent of the other functional groups (FTIR); the measuring error for -S-S-group can be excluded. Carboxylate ions show relatively the least fluctuation. The summary data obtained, involving degreased dried wool, illustrate the complexity of processes running in irradiated wool depending on, until now, undefined variables.

To obtain more information on transformation dynamics of individual species, the measurements were repeated within intervals 88 and 123 days from the exposure, with the samples being kept freely under laboratory conditions. The results for disulphides, S-sulfonate, cystine monoxide, and carboxylates are displayed in Figure 2 and data for cystine dioxide and cysteic acid are shown in Figure 3.

After longer postexposure interval, the enhanced content of disulphides was no longer the case; the sulphides were transformed progressively into S-oxidized products.

As seen in Figure 3, after an 88-day interval, the increase for cysteic acid and cystine dioxide is significantly higher than for other S-species. This finding is in conformity with conclusions of authors dealing with wool plasma treatment [26], wool photodegradation [19], and wool oxidation [30]. The above-mentioned authors considered cysteic acid to be the final transformation product of -S-S- formation and cystine dioxide to be its precursor.

Our measurement of the wool after 123 days from the irradiation definitively confirmed cysteic acid as the final product also in the case of electron beam irradiation (Figures 4 and 5). The dependence in Figure 4 shows negligible content of cystine dioxide beyond 63 kGy dose and a dominant content of cysteic acid (Figure 5).

Besides cysteic acid, also the presence of carboxylate ions in wool is important especially due to interactions with basic groups -NH_2 and isoelectric point setting. More detailed time variations in carboxylate content in the irradiated wool are displayed in Figure 6.

It is apparent that also the carboxylate portion varies not only with absorbed dose but also with time. The fluctuation can be attributed to both generation and following consumption of the carboxylates in intramolecular reactions with acidic groups of keratin, for example, -COO^- with H_3N^+-. Postirradiation time available for intramolecular reactions is one of the decisive factors. Since in the FTIR spectrum isolated -COO^- groups were measured, which does not give a signal identical with the associated ones, after interaction of the carboxylate the corresponding content estimated from the isolated signal should be lower. Development of the -COO^- content after 123 days (Figure 6) shows that, with the exception of the 40 kGy dose, the -COO^- content is under the level of the nonirradiated wool (≤1).

3.2. EPR Spectral Measurements. In general, it is accepted that radiation can provoke the breaking of bonds, polymeric chains, or cross-linking due to mutual recombination of generated free radicals [31–34]. Our EPR spectroscopic observation provided some imagination on the generation of free radicals in the wool after being irradiated by the electron beam. The first EPR measurement was carried out 7 days after the irradiation and then after 1 and 2 months (and partially after 3 months, too). These measurements after these time laps attempt to give information on the occurrence, identity, and lifetime of originally present radicals.

The sample of nonirradiated wool showed an unexpected lightly intensive sharp EPR signal around 3500 Gauss. Using 10 scans, the intensity of the signal was improved and the signal was assigned to the sample cautiously, since some trace impurities in the sample can contribute to the signal. Some scientific sources present such a signal to be due to a melanin radical and can be found in native wool, even in white wool, as a consequence of sunlight [35]. The fact that broad line shape for the native wool was consistent, unlike for the exposed samples, is worth mentioning. A possible explanation for the broad line shape could be the presence of a little amount of iron or copper oxides superposed onto the spectrum. The broad line EPR spectrum of nonirradiated wool (Figure 7(a)) shows some similarity to the EPR spectrum of small quantity of powdery rust (Figure 7(b)).

In wool, iron as well as other metal elements is normally found at trace levels and the content varies according to the origin and breeding conditions of the sheep. Patkowska-Sokoła et al. [36] analysed sheep wools from Poland, Greece, and Syria. They determined iron content within the range around 22–400 mg/kg and copper content of 5–10 mg/kg, respectively, calculated for dry degreased wool. Both elements are EPR active and so expectation of their EPR signals is reasonable. In addition, Fe^{2+}/Fe^{3+} and Cu^+/Cu^{2+} transition systems have catalytic effects, so they can catalyse redox processes in wool. Such reactions would take place in the wool and could explain the unexpected results such as the transitive increase of the disulphide content in the wool 4 days after the exposure (Figure 1). This could influence the dynamics of other species' transformation. The potential catalytic effect of microelements in the wool brings another possible variable into the effect of the electron beam on wool requiring further examination.

In EPR spectra of the all irradiated samples, a narrow singlet line was observed around 3350 Gauss ($g = 2.0$) with a full width of about 25 Gauss and with peak to peak width of approximately 9 Gauss. This is likely to be an organic in origin radical (Figure 8). With reference to published data [35–37], this signal (Figure 8) can be assigned to a melanin radical.

There appears to be a hint of fine structure characteristic of pheomelanins, as opposed to eumelanins, which are present in light hair [38]. However, closer inspection revealed no fine structure, with such fine structure only being visible under special conditions [38]. Regarding the common keratin base of hair and wool, we consider these facts to be indicative for our sample, too. Therefore, we assigned this signal to a radical generated from keratin due to radiation. The radical was within 1-2 months fairly stable but, after 3 months, some decrease was observed in its intensity. We suppose the quenching was connected with transformation into some product and since the samples were stored in open tubes accessible to air oxygen and air humidity the transformed products were predominantly S-oxidation species.

The noticeable exception was for the samples irradiated at high doses of 250 and 350 kGy. The signal ($g = 2.0$) with peak to peak width of 9 Gauss approximately is a little more than 5-6 Gauss mentioned by Mamedov et al. [35] and a little less than what is presented by Zdybel et al. [37]. Initially, the sharp organic in origin radical signal was more visibly quenched already 1 month after irradiation (Figure 9). This may suggest that high doses of irradiation produce additional products which scavenge the free radical. However, such faster quenching of the signal only occurs when exposed to open air and moisture. In contrast, when the wool was stored for 2 months in a closed tube, the signal appeared with intensity similar to the measurements first performed. This may suggest that high radiation doses generated more types of products deactivating the generated radicals possibly through radical recombination mechanisms, too. That fact could be consistent with our previous observations [23] indicating both a moderate cross-linking and chain breaking.

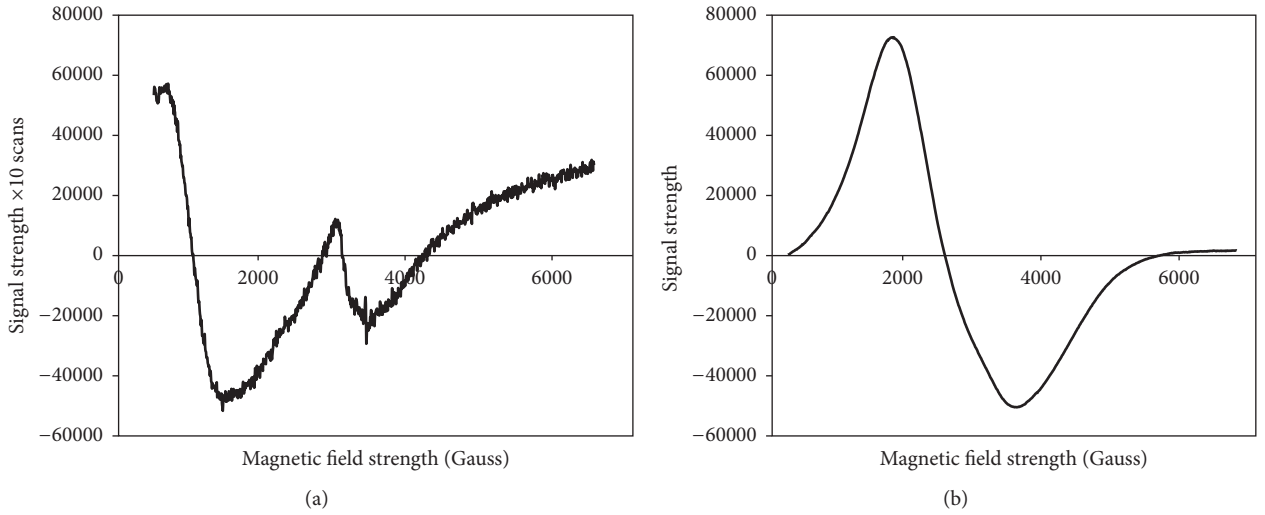

Figure 7: EPR spectra of nonirradiated wool (a) and powdery rust (b).

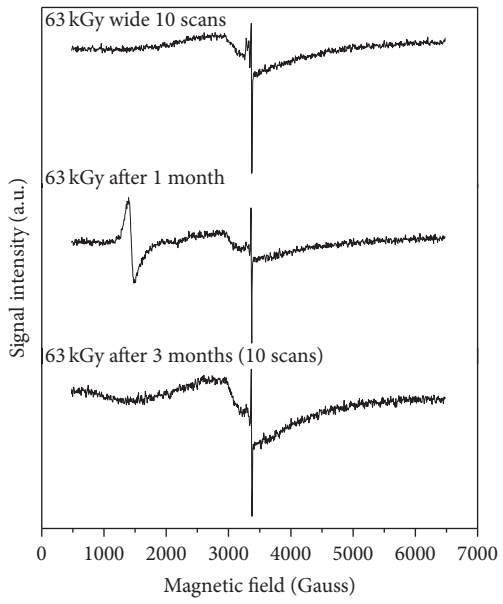

Figure 8: Variation of EPR spectra taken from wool irradiated by electron beam (63 kGy) and measured after time intervals, 7 days, 1 month, and 3 months after irradiation; EPR spectrum parameters: centre of magnetic field, 3350 Gauss, magnetic field amplitude, 1200 Gauss, and resonant frequency, 9.944 GHz, 10 scans.

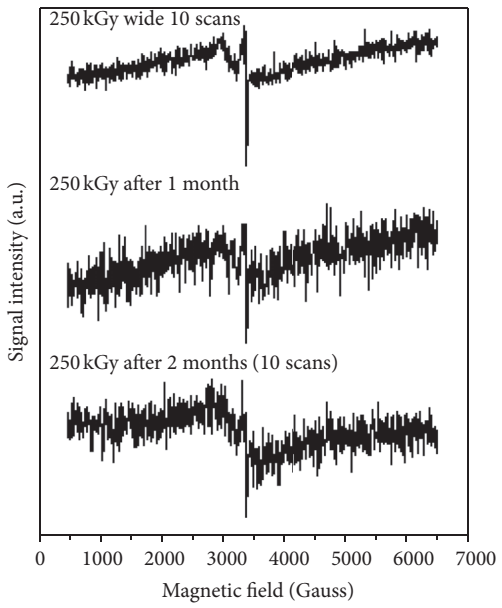

Figure 9: Variation of EPR spectra taken from wool irradiated by electron beam (250 kGy) and measured within time interval from the exposure: 7 days, 1 month, and 2 months; measuring conditions as mentioned in Figure 8.

3.3. Secondary Structure. Beyond our original intention, we additionally tried to utilize the FTIR spectra also for estimation of the secondary structure development for individual absorbed doses with time after irradiation. This approach, based on the differentiation of appropriate amide bands of proteins, was firstly presented in [39]. According to our present knowledge, the related data in scientific sources are rare and mostly deal with wool keratin dissolved and then obtained in solid form with no chemical modification [11, 40, 41], which is not the case of wool in our interest. In general, usable bands are Amide I (1600–1700 cm^{-1}) and Amide II (1510–1580 cm^{-1}). Both bands are conformationally sensitive. The fitting of FTIR spectra converted to second-order derivative into Gaussian components enables us to estimate the

portion of secondary structure conformations (α-helical, β-sheet, and random) in wool samples assigning corresponding portions of the fitted band area from the whole band area. Amide I frequency relates to backbone conformation and characteristics of the hydrogen bonding pattern. Amide II band is more complex than Amide I and involves in-plane N-H bending and C-N and the C-C stretching vibrations [42]. However, some complication can arise from the H-O-H bending mode around 1640 cm^{-1} and affect the band intensity of Amide I [27]. Sheep wool is susceptible to absorbing humidity and the content of absorbed water during experiments is difficult to control. In addition, if chemical changes involving the addition of oxygen into keratin molecules occur, then also the hydrogen bonding pattern has to change with the chemical variations. Thus, the usability of Amide I band in our case becomes doubtful. To avoid this, and especially when Amide I band provided us with somewhat irrational results for the irradiated samples confirming our supposition, we decided to use deconvolution of Amide II band. We are aware that the applied spectral resolution of 8 cm^{-1} is not optimal for Amide II due to some overlapping of individual conformational components within the Amide II band (Table 2), although the resolution would be enough for Amide I deconvolution. On the other hand, this handicap is the same for all measurements and, even under such circumstances, a certain concept of a draft-quality variance in the secondary structure can be deduced (Figure 10). More details and reliable data on the wool secondary structure with absorbed dose and postirradiation time have to be obtained using more sensitive spectral resolution.

Each absorbed dose provoked different effects on the chemical structure of the wool as seen in Figures 1–6. It is thus reasonable to expect that this fact is reflected by a variable secondary structure. In fact, secondary structure pattern changed considerably not only with absorbed dose but also with time (Figure 10). This confirms the complexity of the irradiated wool.

It is not clear yet why measurable variations, although of the least variation, were observable also in nonirradiated wool. Probably the variations are connected with the detected free radical (Figure 7(a)) and its progressive quenching in contact of the wool with room atmosphere inducting an oxidative product.

The portion of α-helix, β-sheet, and random structures changed with every monitored time. Fluctuation in each mentioned conformation attained a maximum up to about 80% and no conformation was dominant within the whole period. Attempts to correlate the observed secondary structure with corresponding evidence of high content of cysteic acid as "reference" product led to inconsistent relations. Applying some approximation, it can be ascertained that for postexposure times of 88 and 123 days there was some connection with the high cysteic acid amount matching, except for the lowest dose of 16 kGy, with increased presence of random or residual structure. This implies that chemical and secondary structures affect each other indicating chemical variation as determining and leading to amorphorization. However, the assigning of the ongoing chemical changes to corresponding composition of the conformations without targeted study would be only speculation.

4. Conclusions

Sheep wool scoured in ultrasonic water bath at 40°C dried at the same temperature and then stored under laboratory conditions without limiting the influence of air and air humidity was irradiated by an accelerated electron beam in air from a 5 MeV source with absorbed doses within 0–350 kGy and at dose rate of 750 kGy/h. Variations of chemical and secondary structure in the wool were measured by FTIR, Raman, and EPR spectroscopy after a short time lapse of being irradiated as well as after longer time intervals. Based on FTIR and Raman spectral results, the reactive products S-sulfonate, cystine monoxide, cystine dioxide, cysteic acid, disulphides, and carboxylates displayed a considerable fluctuation in amount regarding both absorbed dose and time. The pattern of the transformation variations depending on absorbed dose was not identical with that observed for the dry degreased wool in an earlier study [23], indicating a faster start of oxidative product generation with absorbed dose. This acceleration is assigned primarily to the effect of some residual humidity as an oxygen source directly inside the fibres. Mutual transformation of S-oxidized species onto cysteic acid, a dominant product, increased with the time lapse from the sample irradiation of interest to other S-species. As EPR results showed, free radicals generated in the samples irradiated by lower doses are of longer lifetime compared with the radicals induced by higher doses. The latter are believed to be quenched faster due to the contribution of their recombination and/or breaking of macrochains. An observed weak EPR signal in the nonirradiated wool was assigned to melanin radical and possibly some trace amounts of iron present in wool normally together with other microelements which can also affect the monitored transformation processes catalytically. Secondary structure of wool (α-helix, β-sheet, and random conformations) estimated from deconvolution of Amide II band presented massive variability depending on absorbed dose as well as postexposure time indicating no trend. Amorphorization of the wool occurs since oxidized points of the macrochains hinder the formation the regular and thermodynamically favourable α-helical conformation even despite better mobility of chain fragments. With respect to time, the most stable secondary structure is observed logically in nonirradiated wool; however, this also showed a small but observable change after a longer time.

Conflicts of Interest

The authors declare that there are no conflicts of interest regarding the publication of this paper.

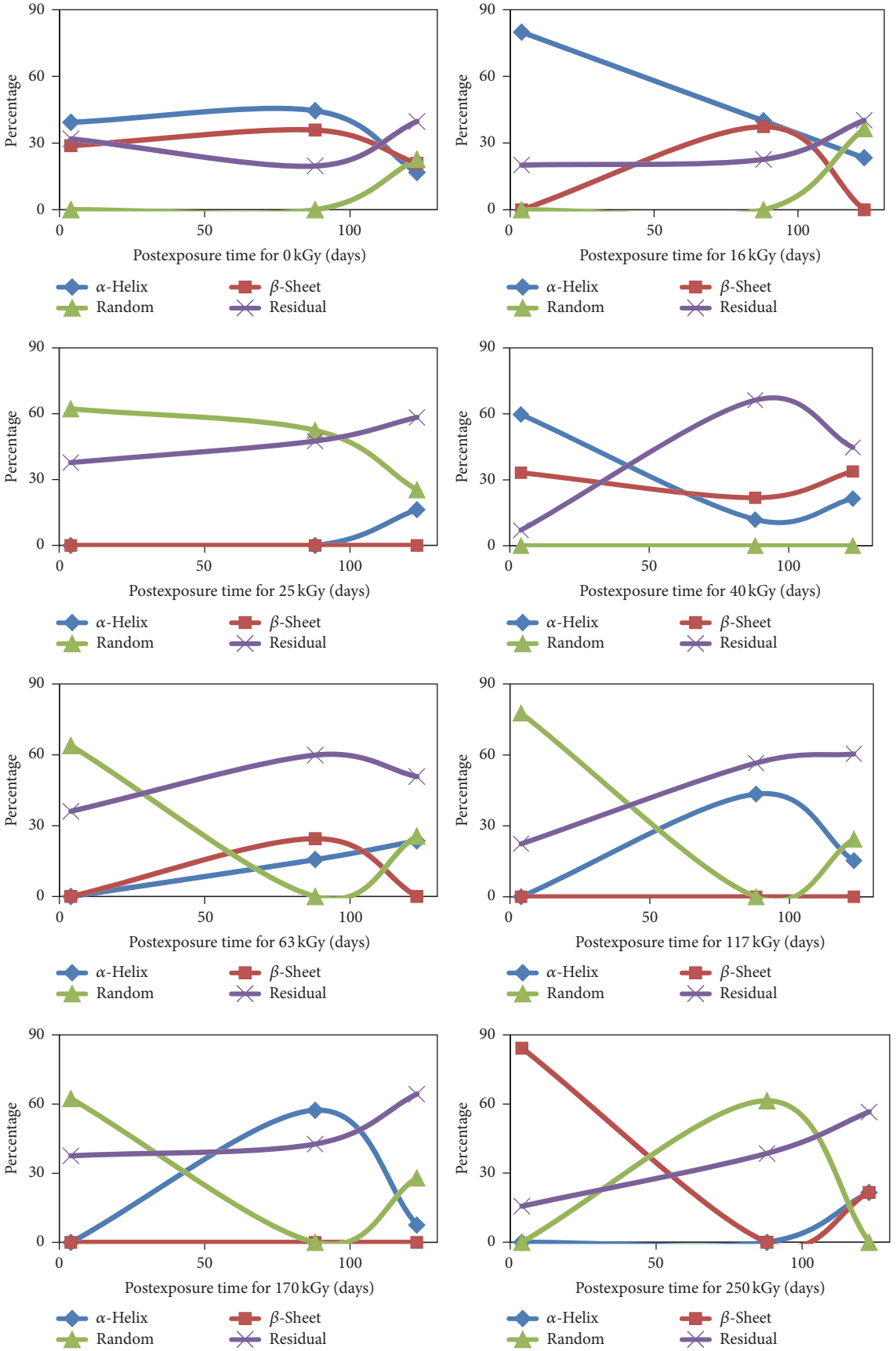

Figure 10: Continued.

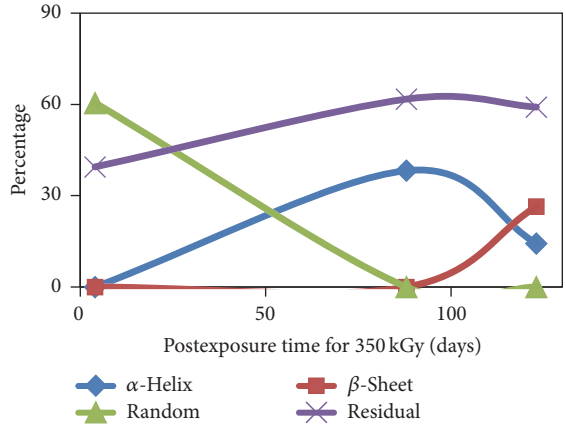

Figure 10: Variations of conformation in the wool secondary structure with absorbed dose and postirradiation time.

Acknowledgments

This work was sponsored by University Grant Agency of Faculty of Natural Sciences, Constantine the Philosopher University in Nitra (Project UGA VIII/5/2016) and by Slovak Research and Development Agency (Project APVV-15-0079). The authors wish to thank Dr. Miroslava Novotná from Central Laboratories at the Institute of Chemical Technology, Prague, Czech Republic, for enabling of FTIR measurement. They also thank Professor Marian Valko from Faculty of Chemical and Food Technology, Slovak University of Technology, Bratislava, Slovakia, for consultations about the EPR interpretations.

References

[1] H. Zhang, S. Deb-Choudhury, J. Plowman, and J. Dyer, "The effect of wool surface and interior modification on subsequent photostability," *Journal of Applied Polymer Science*, vol. 127, no. 5, pp. 3435–3440, 2013.

[2] V. L. Hughes, G. Nelson, and G. East, "Surface modification of cashmere fibers by reverse proteolysis," *AATCC Magazine*, vol. 1, no. 3, pp. 39–43, 2001.

[3] J. S. Church, G. L. Corino, and A. L. Woodhead, "The analysis of merino wool cuticle and cortex with FT Raman spectroscopy," *Biopolymers*, vol. 42, no. 1, pp. 7–17, 1997.

[4] L. J. Hogg, H. G. M. Edwards, D. W. Farwell, and A. T. Peters, "FT Raman spectroscopic studies of wool," *Journal of the Society of Dyers and Colourists*, vol. 110, no. 5-6, pp. 196–199, 1994.

[5] A. Aluigi, C. Vineis, C. Tonin, C. Tonetti, A. Varesano, and G. Mazzuchetti, "Wool keratin-based nanofibres for active filtration of air and water," *Journal of Biobased Materials and Bioenergy*, vol. 3, no. 3, pp. 311–319, 2009.

[6] W. Von Bergen, *Wool Handbook*, vol. 1, John Wiley & Sons, New York, NY, USA, 3rd edition, 1963.

[7] J. A. Rippon, "The structure of wool," in *Wool Dyeing*, D. M. Lewis, Ed., pp. 1–51, Society of Dyers and Colourists, Bradford, UK, 1992.

[8] C. Tonin, A. Aluigi, A. Varesano, and C. Vineis, "Keratin-based nanofibres," in *Nanofibres*, A. Kumar, Ed., p. 348, InTech, Rijeka, Croatia, 2010.

[9] H. Gong, H. Zhou, and J. G. H. Hickford, "Diversity of the glycine/tyrosine-rich keratin-associated protein 6 gene (KAP6) family in sheep," *Molecular Biology Reports*, vol. 38, no. 1, pp. 31–35, 2011.

[10] L. M. Dowling, W. G. Crewther, and D. A. D. Parry, "Secondary structure of component 8c-1 of α-keratin. An analysis of the amino acid sequence," *Biochemical Journal*, vol. 236, no. 3, pp. 705–712, 1986.

[11] J. M. Cardamone, A. Nuñez, R. A. Garcia, and M. Aldema-Ramos, "Characterizing Wool Keratin," *Research Letters in Materials Science*, vol. 2009, Article ID 147175, 5 pages, 2009.

[12] C. W. Kan, W. Y. I. Tsoi, C. W. M. Yuen, T. M. Choi, and T. B. Tang, "Achieving nano-scale surface structure on wool fabric by atmospheric pressure plasma treatment," in *Atmospheric Pressure Plasma Treatment of Polymers: Relevance to Adhesion*, M. Thomas and K. L. Mittal, Eds., chapter 5, pp. 157–173, John Wiley & Sons, Hoboken, NJ, USA, 2013.

[13] Y. J. Hwang, M. G. McCord, J. S. An, B. C. Kang, and S. W. Park, "Effects of helium atmospheric pressure plasma treatment on low-stress mechanical properties of polypropylene nonwoven fabrics," *Textile Research Journal*, vol. 75, no. 11, pp. 771–778, 2005.

[14] K. Chi-wai, C. Kwong, and M. Y. Chun-wah, "The possibility of low-temperature plasma treated wool fabric for industrial use," *Autex Research Journal*, vol. 4, no. 1, pp. 37–44, 2004.

[15] H. U. Poll, U. Schladitz, and S. Schreiter, "Penetration of plasma effects into textile structures," *Surface and Coatings Technology*, vol. 142–144, pp. 489–493, 2001.

[16] C. Kan, K. Chan, C. Yuen, and M. Miao, "Surface properties of low-temperature plasma treated wool fabrics," *Journal of Materials Processing Technology*, vol. 83, no. 1-3, pp. 180–184, 1998.

[17] W. L. Xu, X. L. Shen, X. Wang, and G. Z. Ke, "Effective methods for further improving the wool properties treated by corona discharge," *Sen'i Gakkaishi*, vol. 62, pp. 111–114, 2006.

[18] Z. Xue and H. Jin-xin, "Improvement in dyeability of wool fabric by microwave treatment," *Indian Journal of Fibre and Textile Research*, vol. 36, no. 1, pp. 58–62, 2011.

[19] J. S. Church and K. R. Millington, "Photodegradation of wool keratin: Part I. Vibrational spectroscopic studies," *Biospectroscopy*, vol. 2, no. 4, pp. 249–258, 1996.

[20] Y. L. Qiao, W. F. Yang, Q. F. Zhang, and X. X. Shen, "Research on improving the properties of wool fabric with low-temperature

plasma," *Advanced Materials Research*, vol. 331, pp. 338–341, 2011.

[21] R. Molina, P. Jovančić, D. Jocić, E. Bertran, and P. Erra, "Surface characterization of keratin fibres treated by water vapour plasma," *Surface and Interface Analysis*, vol. 35, no. 2, pp. 128–135, 2003.

[22] A. Ceria, F. Rombaldoni, G. Rovero, G. Mazzuchetti, and S. Sicardi, "The effect of an innovative atmospheric plasma jet treatment on physical and mechanical properties of wool fabrics," *Journal of Materials Processing Technology*, vol. 210, no. 5, pp. 720–726, 2010.

[23] M. Porubská, Z. Hanzlíková, J. Braniša et al., "The effect of electron beam on sheep wool," *Polymer Degradation and Stability*, vol. 111, pp. 151–158, 2014.

[24] Z. Hanzlíková, J. Braniša, P. Hybler, I. Šprinclová, K. Jomová, and M. Porubská, "Sorption properties of sheep wool irradiated by accelerated electron beam," *Chemical Papers*, vol. 70, no. 9, pp. 1299–1308, 2016.

[25] M. Zoccola, A. Montarsolo, A. Aluigi, A. Varesano, C. Vineis, and C. Tonin, "Electrospinning of polyamide 6/modified-keratin blends," *E-Polymers*, Article ID 105, 2007.

[26] C. W. Kan and C. W. M. Yuen, "Surface characterisation of low temperature plasma-treated wool fibre," *Journal of Materials Processing Technology*, vol. 178, no. 1–3, pp. 52–60, 2006.

[27] M. Mori and N. Inagaki, "Relationship between anti-felting properties and physicochemical properties of wool treated with low-temperature plasma," *Research Journal of Textile and Apparel (RJTA)*, vol. 10, pp. 33–45, 2006.

[28] Z. Hanzlíková, J. Braniša, J. Ondruška, and M. Porubská, "The uptake and release of humidity by wool irradiated with electron beam," *Journal of Central European Agriculture*, vol. 17, no. 2, pp. 315–324, 2016.

[29] E. Senoz, R. P. Wool, C. W. McChalicher, and C. K. Hong, "Physical and chemical changes in feather keratin during pyrolysis," *Polymer Degradation and Stability*, vol. 97, no. 3, pp. 297–307, 2012.

[30] F. J. Douthwaite, D. M. Lewis, and U. Schumacher-Hamedat, "Reaction of cystine residues in wool with peroxy compounds," *Textile Research Journal*, vol. 63, no. 3, pp. 177–183, 1993.

[31] Z. Ajji, I. Othman, and J. M. Rosiak, "Production of hydrogel wound dressings using gamma radiation," *Nuclear Instruments and Methods in Physics Research, Section B: Beam Interactions with Materials and Atoms*, vol. 229, no. 3-4, pp. 375–380, 2005.

[32] L. V. Abad, L. S. Relleve, C. T. Aranilla, and A. M. Dela Rosa, "Properties of radiation synthesized PVP-kappa carrageenan hydrogel blends," *Radiation Physics and Chemistry*, vol. 68, no. 5, pp. 901–908, 2003.

[33] A. B. Lugão, S. O. Rogero, and S. M. Malmonge, "Rheological behaviour of irradiated wound dressing poly(vinyl pyrrolidone) hydrogels," *Radiation Physics and Chemistry*, vol. 63, no. 3-6, pp. 543–546, 2002.

[34] A. V. Mondino, M. E. González, G. R. Romero, and E. E. Smolko, "Physical properties of gamma irradiated poly(vinyl alcohol) hydrogel preparations," *Radiation Physics and Chemistry*, vol. 55, no. 5-6, pp. 723–726, 1999.

[35] S. V. Mamedov, B. Akta, M. Cantürk et al., "The ESR signals in silk fibroin and wool keratin under both the effect of UV-irradiation and without any external effects and the formation of free radicals," *Biomaterials*, vol. 23, no. 16, pp. 3405–3412, 2002.

[36] B. Patkowska-Sokoła, Z. Dobrzański, K. Osman, R. Bodkowski, and K. Zygadlik, "The content of chosen chemical elements in wool of sheep of different origins and breeds," *Archiv fur Tierzucht*, vol. 52, no. 4, pp. 410–418, 2009.

[37] M. Zdybel, E. Chodurek, and B. Pilawa, "Free radicals in ultraviolet irradiated melanins and melanin complexes with Cd(II) and Cu(II)—EPR examination," *Journal of Applied Biomedicine*, vol. 13, no. 2, pp. 131–141, 2015.

[38] P. M. Plonka, A. T. Slominski, S. Pajak, and K. Urbanska, "Transplantable melanomas in gerbils (meriones unguiculatus). II: melanogenesis," *Experimental Dermatology*, vol. 12, no. 4, pp. 356–364, 2003.

[39] D. M. Byler and H. Susi, "Examination of the secondary structure of proteins by deconvolved FTIR spectra," *Biopolymers*, vol. 25, no. 3, pp. 469–487, 1986.

[40] J. M. Cardamone, "Investigating the microstructure of keratin extracted from wool: peptide sequence (MALDI-TOF/TOF) and protein conformation (FTIR)," *Journal of Molecular Structure*, vol. 969, no. 1–3, pp. 97–105, 2010.

[41] E. Wojciechowska, A. Włochowicz, and A. Wesełucha-Birczyńska, "Application of Fourier-transform infrared and Raman spectroscopy to study degradation of the wool fiber keratin," *Journal of Molecular Structure*, vol. 511-512, pp. 307–318, 1999.

[42] A. Jabs, "Determination of secondary structure in proteins by Fourier transform infrared spectroscopy (FTIR)," http://jenalib.fli-leibniz.de/ImgLibDoc/ftir/IMAGE_FTIR.html.